J. Membrane Biol. 142, 161–170 (1994)

The Journal of
Membrane
Biology

Phenylglucosides and the Na^+/Glucose Cotransporter (SGLT1): Analysis of Interactions

M.P. Lostao, B.A. Hirayama, D.D.F. Loo, E.M. Wright
Department of Physiology, UCLA School of Medicine, 10833 Le Conte Avenue, Los Angeles, California, 90024-1751

Received: 31 May 1994/Revised: 13 July 1994

Abstract. Phenylglucosides are transported by the intestinal Na^+/glucose cotransporter (SGLT1) and phlorizin, the classical competitive inhibitor of SGLT1, is also a phenylglucoside. To investigate the structural requirements for binding of substrates to SGLT1, we have studied the interactions between phenylglucosides and the cotransporter expressed in *Xenopus* oocytes using tracer uptake and electrophysiological methods. Some phenylglucosides inhibited the Na^+-dependent uptake of ^{14}C-α-methyl-D-glucopyranoside (αMDG) with apparent K_is in the range 0.1 to 20 mM, while others had no effect. Electrophysiological experiments indicated that phenylglucosides can act either as: (1) transported substrates, e.g., arbutin; (2) nontransported inhibitors, e.g., glucosylphenyl-isothiocyanate; or (3) noninteracting sugars, e.g., salicin. The transported substrates (glucose, arbutin, phenylglucoside and helicin) induced different maximal currents, and computer simulations showed that this may be explained by a difference in the translocation rates of the sugar and Na^+-loaded transporter. Computational chemistry indicated that all these β-phenylglucosides have similar 3-D structures. Analysis showed that among the side chains in the *para* position of the phenyl ring the –OH group (arbutin) facilitates transport, but the –NCS (glucosylphenyl-isothiocyanate) inhibits transport. In the *ortho* position, $-CH_2OH$ (salicin) prevents interaction, but the aldehyde (helicin) permits the molecule to be transported. Studies such as these may help to understand the geometry and nature of glucoside binding to SGLT1.

Key words: Na^+/glucose cotransporter — *Xenopus* oocytes — Phenylglucosides — Voltage clamp — Kinetics — Molecular modeling

Correspondence to: M.P. Lostao

Introduction

The sugar specificity of the intestinal brush border Na^+/glucose cotransporter has been extensively studied over the past three decades using both in vivo and in vitro intestinal preparations. In the case of the monosaccharides it is clear that D-glucose has the optimal structure, and the minimum requirement is a hexose with an equatorial hydroxyl group on C-2 (*see* Kimmich, 1981; Hopfer, 1987). Furthermore, it was established that bulky substituent residues are only tolerated at carbon C-1, e.g., 4-hydroxyphenyl-β-D-glucopyranoside (arbutin) is transported (Alvarado & Crane, 1964). However, if the residue is too bulky, the glucopyranoside may become a blocker of sugar transport, e.g., phlorizin (phloretin-2-β-D-glucopyranoside) is a high affinity competitive inhibitor. It is not clear if disaccharides such as lactose and sucrose can be transported, as these are digested to free sugars in the gut lumen by pancreatic amylases and brush border carbohydrases.

With the cloning of the major intestinal brush border Na^+/glucose cotransporter (SGLT1, Hediger et al., 1987), its expression in heterologous systems such as *Xenopus* oocytes (Ikeda et al., 1989), and the development of rapid, simple assays for sugar transport in this system (Umbach, Coady & Wright, 1990; Birnir, Loo & Wright, 1991), we have decided to investigate the specificity and kinetics of SGLT1 for phenylglucopyranosides. Our goal was to examine the molecular interactions between glucosides and the Na^+/glucose cotransporter. We have found that several phenylglucopyranosides are transported by SGLT1, but at maximal rates lower than those for the hexoses, and subtle changes in the substituent on the phenyl ring convert the glucopyranosides from transported substrates to inhibitors to noninteracting molecules. Molecular modeling of the glucopyranosides provides insight into the interaction of sugars with the transport protein.

Materials and Methods

Oocyte Preparation

Oocytes were obtained from adult *Xenopus laevis* as previously described (Birnir et al., 1991). They were injected with 50 ng of mRNA coding for the rabbit intestinal Na^+/glucose cotransporter (SGLT1, Hediger et al., 1987) or diethylpyrocarbonate treated-H_2O, and were maintained at 18°C in a Barth's medium containing (in mM): 88 NaCl, 1 KCl, 0.33 $Ca(NO_3)_2$, 0.41 $CaCl_2$, 0.82 $MgSO_2$, 2.4 $NaHCO_3$, 10 HEPES-Tris, 0.1 mg/ml gentamycin, pH 7.4.

Phenylglucosides

All sugars were obtained from Sigma Chemical (St. Louis, MO), namely: D-glucose; α-methyl-D-glucopyranoside (αMDG); 4-hydroxyphenyl-β-D-glucopyranoside (arbutin); phenyl-β-D-glucopyranoside (PG); 2-[hydroxy-methyl]-phenyl-β-D-glucopyranoside (salicin); salicil-aldehyde-β-D-glucopyranoside (helicin); β-D-glucopyranosyl-phenyl-isothiocyanate (GPITC); 4-β-D-glucopyranosyl-aminobenzenesulfonamide (GSA), *p*-nitrophenyl-β-D-glucopyranoside (NPG); phloretin-2-β-D-glucopyranoside (phlorizin, Pz); *p*-nitrophenyl-β-D-mannopyranoside (NPM), β-L-fucopyranosyl-phenyl-isothiocyanate (FPITC); and the disaccharides lactose, trehalose, gentiobiose and isomaltose. All phenylglucosides used were in the β configuration since preliminary experiments showed that α-phenylglucosides did not appear to interact with SGLT1. For convenience, the sugar structures are shown in Fig. 8. Purity was analyzed by HPLC (La Course, Mead & Johnson, 1990; Mopper et al., 1992). Neither glucose nor galactose were detected in arbutin, PG and helicin within a detection limit of 0.002 mol percent. Gentiobiose and isomaltose contained 0.74 and 0.35 mol percent of glucose, respectively.

Uptake Experiments

Sugar uptake was measured by a radiotracer method (Ikeda et al., 1989). Groups of 6–9 oocytes were incubated for 1 hr at 22°C in 500 ml of Na^+ buffer containing 50 μM ^{14}C-α-methylglucoside (2 μCi/ml) in the absence or presence of phenylglucoside. The Na^+-buffer solution contained (in mM): 100 NaCl, 2 KCl, 1 $CaCl_2$, 1 $MgCl_2$ and 10 HEPES/Tris, at pH 7.5. After the incubation period, the ^{14}C content of each oocyte was determined by liquid scintillation counting. Uptakes were expressed as pmol/oocyte hr.

Electrophysiology Experiments

All experiments were performed using the two microelectrode voltage clamp method as described previously (Birnir et al., 1991; Parent et al., 1992*a*). The membrane potential (V_m) was normally held at −50 mV. To obtain current/voltage (*I/V*) relationships, 11 pulses of potential between +50 and −150 mV (−20 mV decrement) were applied using the software CLAMPEX from pCLAMP (Axon Instruments, Foster City, CA). The steady-state sugar-dependent currents were obtained for each voltage as the difference between the current measured at steady-state (>70 msec) in the presence and absence of glucoside. The experiments were performed at 22°C. The apparent affinity ($K_{0.5}$) and the maximal current for sugar (i_{max}) were obtained by fitting the steady-state currents (i) at each membrane potential to the equation:

$$i = i_{max} \cdot [s]/(K_{0.5} + [s]) \quad (1)$$

using the software Enzfitter (version 1.05, Elsevier-Biosoft, Cambridge, United Kingdom), where [*s*] is the extracellular substrate concentration, i_{max} is the apparent maximal current for saturating substrate concentrations and $K_{0.5}$ is the substrate concentration at 50% i_{max}. The presteady-state currents associated with the cotransporter in the absence of substrate, i_2, at time *t* were isolated using the fitted method (Loo et al., 1993) so that

$$i_2 e^{-t/\tau 2} = i_t - i_1 e^{-t/\tau 1} - i_{ss}, \quad (2)$$

where τ_2 is the time constant of the cotransporter current, i_t is the total current at time *t*, i_i is the capacitance current at time *t* with a time constant τ_1, and i_{ss} is the steady current. The charge movement, at each membrane potential, was calculated by integrating the presteady-state currents, and the apparent maximum charge (Q_{max}) was estimated as the difference in charge between the depolarizing and hyperpolarizing limits (+50 and −150 mV, respectively).

GPITC Inhibition of Intestinal Na^+/Glucose Transport

Rabbit intestinal brush border membrane vesicles (BBMV) were prepared (Stevens, Ross & Wright, 1982) and suspended in a phosphate-buffered saline (in mM, 100 NaCl, 2 KCl, 1 $CaCl_2$, 10 phosphate, pH 7.4). BBMV were incubated for 40 min at 22°C at a protein concentration of 2 mg/ml in either 0 or 2 mM GPITC and 0 or 50 mM D-glucose. At the end of the incubation time, the vesicles were washed three times by centrifugation in 300 mM mannitol, buffered to pH 7.4 with 10 mM Tris-HEPES. Initial rates of 50 μM ^{3}H-D-glucose uptake were measured at 3 sec using a rapid filtration assay. Na^+-dependent rates were calculated as the difference between 100 mM NaCl and KCl uptakes.

Computational Chemistry

The optimized three-dimensional structures of the phenylglucosides were obtained using the molecular modeling program Hyperchem (version 2.0, Autodesk, Sausalito, CA). Each structure was created in Hyperchem and, after an initial geometry optimization using the MM+ forcefield, the most favorable configuration (minimum energy configuration) was determined by (i) examining the energy of all structures generated by sequential nested rotation in torsion (20–60 degrees per rotation/bond) about all rotatable bonds, and (ii) optimizing the geometry of the 100 lowest energy configurations of each phenylglucoside. The lowest energy configurations generated by these manipulations represent the most favorable structures for each compound in vacuo. A search of additional optimal structures, other than those generated by the above protocol, using a high-temperature dynamics and annealing simulation, revealed no new structures. Comparison of phenylglucoside structures was performed using Alchemy III (Tripos, St. Louis, MO). In all cases, five atoms in each phenylglucoside were paired (glucose C–2, O–2, C–1, O–5 and glycosidic O–1) in a least square fitting routine. The superimposed structures were then examined for the geometry of the various groups.

Of the compounds tested, published X-ray crystal structures are available for salicin, PG, lactose and trehalose (Cambridge Crystallographic Data Base). The calculated 3-D structures closely resemble the crystal structures for these four sugars.

Results

Uptake Experiments

The first approach to examine the interaction of the phenylglucosides (Fig. 8) with SGLT1 was to study their

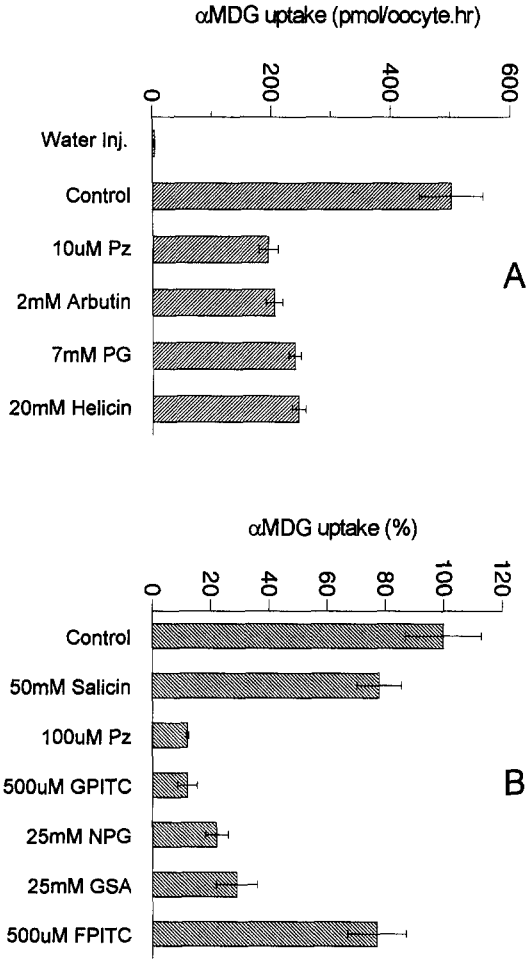

Fig. 1. Na^+-dependent uptake of αMDG in the absence (control) and presence of phenylglucosides. Rabbit SGLT1 mRNA 50 ng was injected into oocytes and the uptake of 50 μM ^{14}C-α-methylglucoside was measured three days later. Uptakes represent the mean of 6–9 measurements and the error bars indicate standard errors. The results shown in *A* were obtained in one experiment and those in *B* were from several experiments normalized to the uptakes in the absence of phenylglucosides. The presence of the indicated concentrations of phenylglucosides inhibits αMDG uptake by 50–90%.

specificity by competition experiments. Preliminary studies, using different concentrations of phenylglucosides, showed that all the phenylglucosides except salicin, inhibited αMDG uptake and provided an estimate of their K_i. Figure 1 shows the uptake of 50 μM αMDG into oocytes in the presence of various phenylglucosides. In control conditions (absence of phenylglucosides) αMDG uptake was 501 ± 53 pmol/oocyte hr, whereas the H_2O injected oocytes did not show Na^+-dependent uptake (Fig. 1*A*). The addition of 10 μM phlorizin, 2 mM arbutin, 7 mM phenylglucoside and 20 mM helicin inhibited αMDG uptake between 50 and 60%. These results suggested a sequence of apparent affinities of: phlorizin > arbutin > PG > helicin. In Fig. 1*B* the concentrations of phenylglucosides produced inhibitions of αMDG uptake

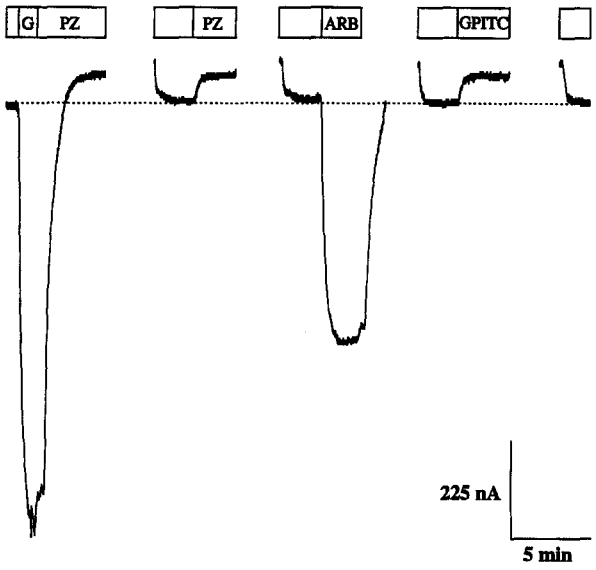

Fig. 2. Na^+ currents generated by SGLT1 in the presence of different sugars. An mRNA-injected oocyte was voltage-clamped at −100 mV in Na^+-buffer solution. The dotted line corresponds to the baseline current (−225 nA) measured in the absence of sugar (blank boxes). Addition of 5 mM D-glucose (*G*) or arbutin (*ARB*) induces an inward Na^+ current shown as a downward deflection of the current trace. Phlorizin (*Pz*) 100 μM inhibits the glucose-induced inward current and, in the absence of sugar, both 100 μM Pz and 1 mM GPITC block the Na^+-leak current, shown as an upward deflection of the current trace. Between trials, the substrates were removed by washing in Na^+-free buffer. After washing, the original Na^+ baseline level was restored.

between 70 and 90%. The sequence of apparent affinities in this case was phlorizin > GPITC ≥ GSA, NPG. Salicin, even at the high concentration of 50 mM, did not significantly affect the uptake of 50 μM αMDG (78 ± 7.7% *vs.* 100 ± 13%). Note in Fig. 1*B* that FPITC was a poor inhibitor relative to GPITC.

Electrophysiology Experiments

Steady-State and Leak Currents

To determine the nature of these inhibitory effects, we measured the steady-state currents generated by glucose and each of the phenylglucosides. Figure 2 shows a continuous current record from a single SGLT1-expressing oocyte, with the membrane potential (V_m) clamped at −100 mV. In the absence of sugar the baseline current was −225 nA. Addition of 5 mM D-glucose induced a rapid inward Na^+ current of −990 nA (first panel) that was blocked and reduced below baseline by 100 μM phlorizin (−35 nA) as previously described (Umbach et al., 1990). In the absence of sugar, phlorizin also reduced the baseline current and the effect was reversible, as shown in the second panel. This phlorizin-sensitive current is referred to as the Na^+-leak current through

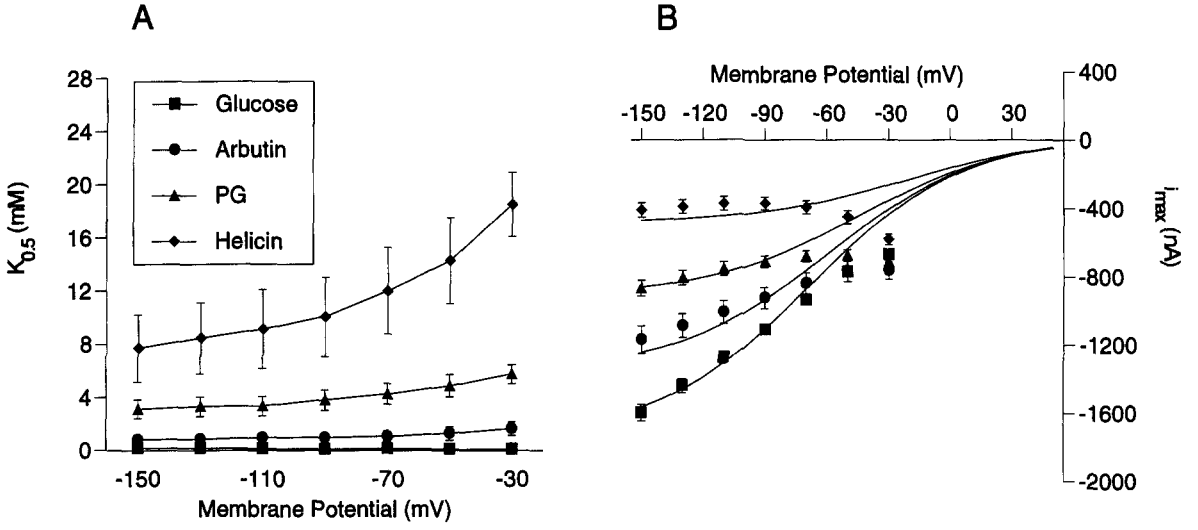

Fig. 3. Voltage dependence of $K_{0.5}$ and i_{max} of transported phenylglucosides. Experiments were performed on one mRNA-injected oocyte three days after injection. The holding potential was −50 mV. For each glucoside, $K_{0.5}$ and i_{max} were obtained at every membrane potential by fitting the steady-state currents obtained at six different concentrations (0.1–50 mM) to Eq. (1). The error bars correspond to the error in the fitting. (*A*) $K_{0.5}/V$ curves. (*B*) i_{max}/V curves. The kinetic model of SGLT1 (Parent et al., 1992*b*) was used to examine the step(s) in the process affected by the glucose analogues. The predicted curves (continuous line) were obtained with different k_{34} constants values for each glucoside: 50, 25, 12 and 5 sec^{-1} for glucose, arbutin, PG and helicin, respectively.

SGLT1 (Umbach et al., 1990; Parent et al., 1992*a,b*). The third panel shows that arbutin induced an inward Na^+ current (−560 nA), indicating that it is a substrate for SGLT1. On the contrary, GPITC (fourth panel) did not induce inward Na^+ current. Instead, it inhibited the baseline current in a manner similar to that of phlorizin, reducing the Na^+ leak and indicating that it is an inhibitor of SGLT1. Two other phenylglucosides, PG and helicin, induced inward Na^+ currents, whereas NPG and GSA inhibited the Na^+ leak.

The effect of the membrane potential on the apparent kinetic constants of SGLT1 for glucose or transported phenylglucosides is shown in Fig. 3. Substrate-dependent steady-state currents were fitted to Eq. (1) to estimate $K_{0.5}$ and i_{max} for each substrate. Consistent with previous studies (Umbach et al., 1990; Birnir et al., 1991), the i_{max} for glucose increased with hyperpolarization from −673 nA at V_m = −30 mV to −1,600 nA at V_m = −150 mV, whereas $K_{0.5}$ was relatively independent of voltage (0.11 mM at V_m = −30 mV, 0.16 mM at V_m = −150 mV). The phenylglucosides' $K_{0.5}$ showed a greater sensitivity to V_m than the glucose $K_{0.5}$, decreasing by a factor of 2 or more from V_m = −30 to −150 mV. The $K_{0.5}$ for arbutin decreased from 1.6 mM at V_m = −30 to 0.8 mM at V_m = −150 mV. Similarly the $K_{0.5}$ for PG and helicin also decreased from 5.7 and 18 mM, respectively, at V_m = −30 mV to 3.1 and 7.7 mM at V_m = −150 mV. On the other hand, the sensitivity of i_{max} to V_m was lower, so that over the range of V_m = −30 to −150 mV i_{max} for arbutin only increased from −763 to −1,170 nA, compared to the almost threefold increase observed with glucose. Values of i_{max} calculated for PG and helicin showed almost no sensitivity to V_m, with i_{max} for PG increasing from −711 to −868 nA, and decreasing from −581 to −410 nA for helicin.

Examples of the *I/V* curves for a substrate and a blocker are shown in Fig. 4. Substrates such as arbutin induce inward Na^+ currents which are sensitive to V_m, increasing with increasing hyperpolarization. Inhibitors, such as GPITC, by inhibiting the Na^+ leak, appear to induce net outward currents.

The molecular properties which make one compound a substrate and another a blocker may not be absolute. When the concentration of a blocker is increased far beyond its K_i, its blockage of the Na^+ leak becomes incomplete. Figure 5 shows an experiment in which the concentration of phlorizin (K_i = 10 μM) was increased from 5 μM to 1 mM. The Na^+-leak current decreased as phlorizin concentration increased from 5 to 100 μM. When the phlorizin concentration was further increased to 1 mM, however, an inward current, relative to the values observed at 100 μM, was measured. This may represent a low level of transport of phlorizin via SGLT1. A similar pattern was observed for the other blockers, GPITC, NPG and GSA. At V_m = −150 mV, 0.5 mM GPITC, 5 mM GSA or 25 mM NPG inhibited the Na^+ leak by 472, 214 and 279 nA, respectively. When the inhibitor concentrations were raised to 10 mM GPITC, 30 mM GSA or 50 mM NPG the inhibition was 281, 36 and 96 nA, respectively. At a concentration of 50 mM and membrane potential from −90 to −150 mV, salicin inhibited the Na^+-leak current 125 nA, i.e., only about half that recorded with 100 μM phlorizin.

In control experiments, analogues of sugars which

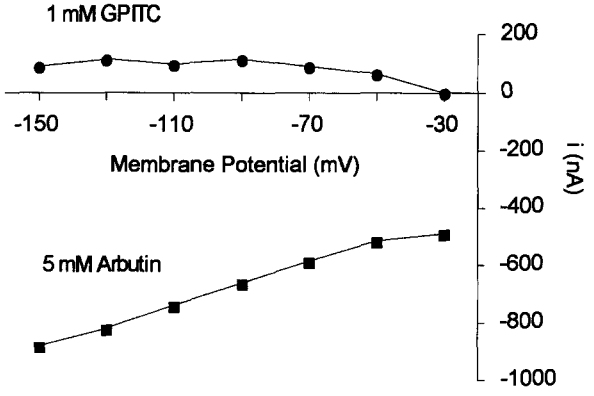

Fig. 4. Steady-state current-voltage relationship of the current generated by arbutin and glucosylphenyl-isothiocyanate. The arbutin curve corresponds to the experiments performed for Fig. 3. The curve for GPITC was obtained in a different oocyte from the same batch, four days after mRNA injection. The holding potential was −50 mV. The currents were obtained subtracting the current generated in the absence and presence of the phenylglucoside. Arbutin 5 mM produces inward current and 1 mM GPITC blocks the Na^+-leak current as shown by the positive current values.

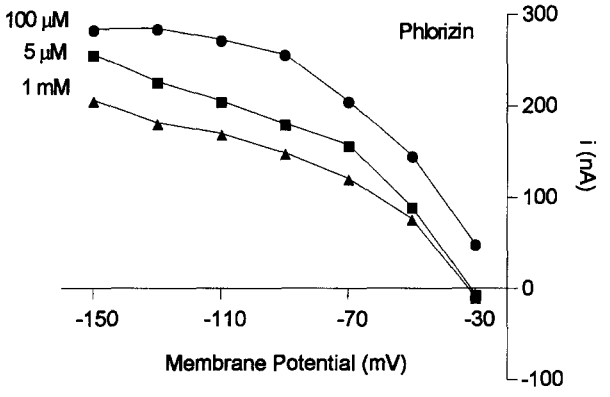

Fig. 5. Effect of phlorizin concentration on the Na^+-leak current. Steady-state *I/V* curves at each concentration were obtained by subtracting from the current in the presence of phlorizin the current in its absence before adding phlorizin to the extracellular solution. The positive current indicates inhibition of the Na^+-leak current. Phlorizin 1 mM produces lower inhibition than 100 and 5 µM.

are not substrates of SGLT1, 500 µM L-fucosylphenyl-isothiocyanate and 25 mM *p*-nitrophenyl-D-mannoside, were tested for effects on tracer αMDG uptake into oocytes. Neither of these sugars nor 15 mM sulfanilamide had any effect (Fig. 1*B* shows the effect of FPITC). We also found that disaccharides did not interact with SGLT1. Lactose and trehalose did not inhibit αMDG uptake nor generated inward Na^+ current or block Na^+-leak pathway. Other disaccharides such as gentiobiose and isomaltose were tested, but the inhibition of αMDG uptake and the inward currents they generated were due to glucose contamination.

SGLT1 Charge Movement

As reported previously (Loo et al., 1993), SGLT1 in the absence of sugar exhibits transient currents after voltage steps in the membrane potential. These currents are due to SGLT1 charge movements (Q), and Q_{max} is directly proportional to the number of transporter molecules expressed in the membrane (Zampighi et al., 1994). To further investigate the interaction of phenylglucosides with SGLT1, we measured their effect on charge transfer. In Fig. 6, Q_{max} was 68 ± 3 nC in the absence of sugar. D-glucose, transported phenylglucosides and blockers all reduced Q_{max} with a potency comparable to their apparent $K_{0.5}$ and K_i (*compare* Figs. 6, 1 and 3*A*); e.g., 10 mM arbutin inhibited Q_{max} by 60% and 0.1 mM GPITC by 80%. As may be anticipated, 50 mM salicin did not block charge transfer.

Brush Border Membrane Experiments

In our electrophysiological experiments the effects of GPITC were reversible. This is perhaps surprising in view of the covalent modification of lysine residues in proteins by phenyl-isothiocyanates. We further explored the effect of GPITC on SGLT1 using brush border membrane vesicles. Figure 7 shows that treatment of brush border membranes with 2 mM GPITC for 40 min irreversibly blocked Na^+-dependent glucose transport by greater than 90%. However, adding 50 mM D-glucose during the exposure of the membranes to GPITC protected against this irreversible inhibition. These results suggest that GPITC interactions with SGLT1 becomes irreversible after long exposure (40 *vs.* 5 min).

Structural Comparison

Our experiments show that phenylglucosides may be divided into three groups (Fig. 8): (1) transported substrates for SGLT1, (2) blockers of SGLT1 and (3) non-interacting molecules. Using the Hyperchem molecular modeling program, we built the 3-D structures of the phenylglucosides and systematically searched to find the most favorable (lowest energy) configurations as described in Materials and Methods. After overlaying the optimized 3-D structures (Fig. 9), we found that the relative positions of the rigid phenyl ring were comparable. The phenyl ring of the transported substrates and salicin superimpose well (Fig. 9*A*). The conjugation of the phenyl ring to glucose decreases the apparent affinity from 0.12 mM (glucose) to 5 mM (PG), whereas the addition of hydroxyl group to the ring in the *para* position increases the apparent affinity to 1.3 mM (arbutin). A –CHO group in the *ortho* position decreases the apparent affinity to 14 mM (helicin) and $-CH_2OH$ group produces a nonreactive compound (salicin). The phenyl ring closely superim-

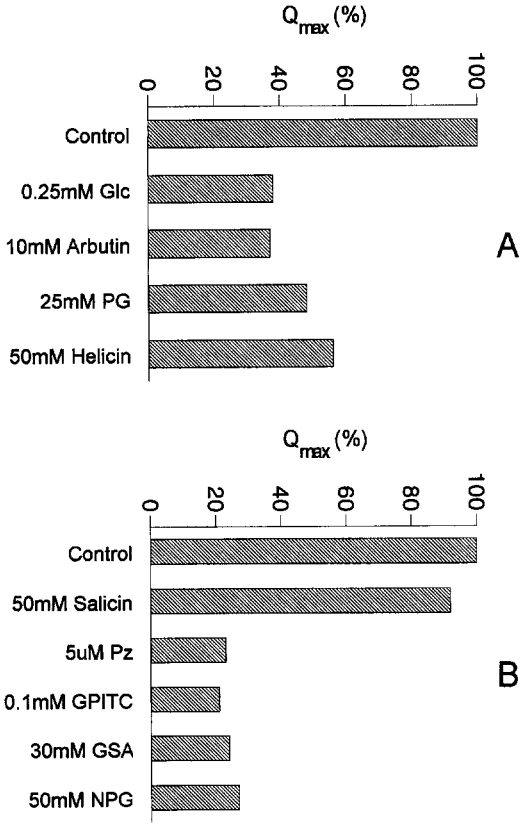

Fig. 6. Effect of the phenylglucosides on Q_{max}. Same oocytes as in Fig. 3 for transported glucosides and as in Fig. 4 for blockers. The oocytes were held at −50 mV and the membrane stepped to 11 potential pulses as indicated in Materials and Methods. For each membrane potential, Q was obtained from the integration of the transient currents during the on response and Q_{max} determined as the difference in Q between the depolarizing and hyperpolarizing limits (+50 and −150 mV, respectively). Q_{max} in control conditions was 68 ± 3 nC. Both the transported glucosides and the blockers reduced Q_{max}. (*A*) Effect of the transported sugars. (*B*) Effect of the blockers.

poses in GPITC, arbutin and NPG (Fig. 9*B*), hence, differences in the character of the group must explain the distinct behavior of these three glucosides with *para* substitutions. GSA and NPG phenyl rings do not overlie completely due to the three torsion angles between glucose and the sulfanilamide group in GSA, which orient the rings in different directions (Fig. 9*C*). However, both sugars show similar apparent affinities for SGLT1 (K_i ~ 20 mM). In Fig. 9*D*, the position of the first phlorizin phenyl ring is close to that of the helicin ring so that the –CHO group in the *ortho* position of both molecules has the same relative position as the $-CH_2OH$ group in salicin. The two molecules may interact with SGLT1 through this chemical group, but the small size of helicin allows it to be transported, whereas the bulky size of phlorizin and the interactions of the hydroxyl groups may prevent it from being transported. From this comparison, it is clear that both the nature of the side chain

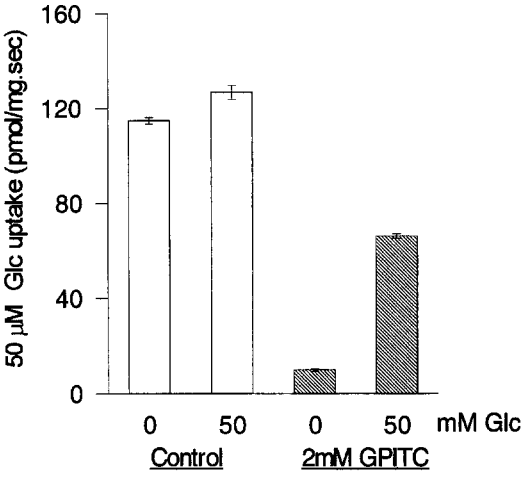

Fig. 7. Na^+-dependent glucose uptake into brush border membrane vesicles: substrate protectable inhibition by GPITC. Rabbit intestinal brush border vesicles were incubated with 2 mM GPITC, as described in Materials and Methods, in 0 or 50 mM glucose. At the end of the incubation time, uptake of 50 µM ^{3}H-D-glucose was measured at 3 sec. Glucose was able to protect SGLT1 from covalent inhibition by GPITC. Uptakes represent the mean of three estimates and the error bars indicate standard errors.

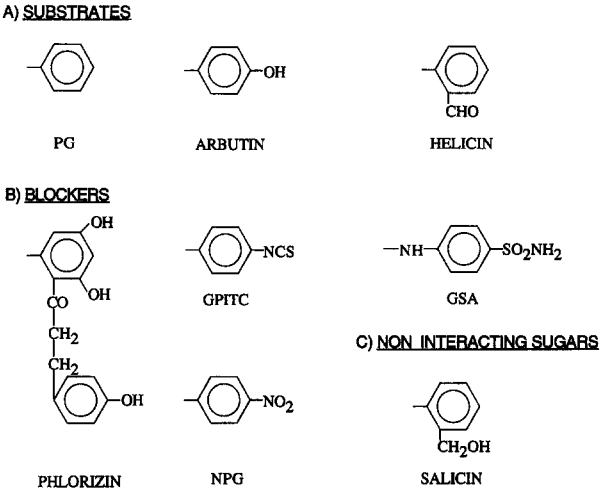

Fig. 8. Chemical structure of the phenyl ring of the glucosides used in the study. All sugars are β-D-phenylglucosides.

and its position on the phenyl ring are a determining factor in substrate interaction with SGLT1.

Discussion

Phenylglucosides Kinetics

According to their properties, the sugars can be classified into three groups: (1) transported sugars (arbutin, PG, helicin), since they induce inward Na^+ current and inhibit

αMDG uptake; (2) blockers or nontransported inhibitors (GPITC, NPG, GSA), since they inhibit αMDG uptake and the Na^+-leak current and do not induce inward Na^+ currents, and (3) noninteracting sugars (salicin, FPITC, NPM, disaccharides, α-phenylglucosides) which do not inhibit αMDG uptake, do not generate inward Na^+ current nor block the Na^+-leak current.

The transported phenylglucosides showed lower apparent affinities than D-glucose: $K_{0.5}$ between 1–14 mM for phenylglucosides *vs.* 0.1 mM for glucose at −50 mV membrane potential (Fig. 3*B*). These results agree with previous studies on rat and hamster intestinal tissue which showed that arbutin, PG and helicin were transported by the intestinal Na^+/glucose cotransporter (Landau, Bernstein & Wilson, 1962; Alvardo & Crane, 1964). The apparent $K_{0.5}$s for arbutin (2 mM) and PG (2–4 mM) are comparable to those obtained here (in Fig. 3*A*, $K_{0.5}$s for arbutin and PG, respectively, are 1.3 and 4.9 mM). The voltage dependence of $K_{0.5}$ and i_{max}, a characteristic of the monosaccharide substrates of SGLT1 (Umbach et al., 1990; Birnir et al., 1991; Parent et al., 1992*a*), was also observed for these transported phenylglucosides (Fig. 3). Glucose, arbutin and PG apparent $K_{0.5}$s exhibit only a slight voltage dependence, whereas helicin shows a voltage dependence comparable to that for monosaccharide at low external Na^+ concentrations. The i_{max} values for these transported phenylglucosides were lower and less voltage dependent than for D-glucose between −50 and −150 mV (Fig. 3*B*). This is unlike that obtained for monosaccharides where the i_{max} and the i_{max}/voltage curves were independent of the sugar (Birnir et al., 1991). That the i_{max}s for the phenylglucosides were lower than for the monosaccharides, especially at hyperpolarizing potentials, suggests that the bulky phenyl residues impede the translocation of the sugar across the membrane. According to the kinetic model proposed for Na^+/glucose cotransport (Parent et al., 1992*b*), this step is the isomerization of the fully loaded sugar/Na_2/carrier complex from the outward (SNa_2C') to the inward (SNa_2C'') facing conformation, i.e.,

$$SNa_2C' \underset{k_{43}}{\overset{k_{34}}{\rightleftarrows}} SNa_2C'', \qquad where\ k_{34} = k_{43}$$

In fact, reduction in the rate constants for the isomerization (k_{34},k_{43}) can account for the observed i_{max} values between −60 and −150 mV for all three phenylglucosides (Fig. 3*B*). These values are 50, 25, 12 and 5 sec^{-1} for glucose, arbutin, PG and helicin, respectively. Between −30 and −60 mV the fit of the data to the model is rather poor. This is probably due to uncertainty about rate constants for Na^+ and sugar dissociation and association at the cytoplasmic surface of the membrane, and a shift in the rate-limiting step with voltage (*see* Parent et al., 1992*b*).

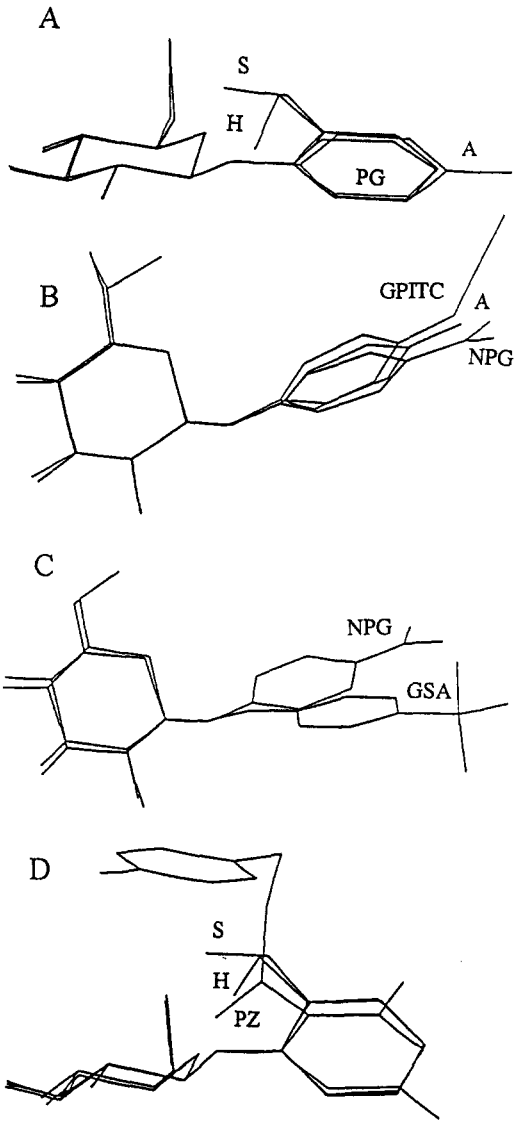

Fig. 9. Superimposition of the three-dimensional structure of the phenylglucosides. The 3-D structures and their superimposition were obtained using Hyperchem and Alchemy molecular modeling programs, respectively. Hydrogen atoms are removed from all the structures for clarity. (*A*) PG, arbutin (*A*), helicin (*H*) and salicin (*S*); (*B*) GPITC, NPG and arbutin; (*C*) NPG and GSA; (*D*) phlorizin, helicin and salicin. Note that the phenyl-β-D-glucopyranose framework provides a constant platform.

Our results also showed that besides phlorizin, other phenylglucosides can act as nontransported inhibitors of SGLT1 since they inhibit αMDG uptake and do not induce inward Na^+ current. Furthermore, these phenylglucoside inhibitors block the Na^+ leak pathway through SGLT1 in the absence of sugar like phlorizin (Umbach et al., 1990). With apparent K_is ranging from less than 0.5 to 20 mM, the inhibitory effect is specific for the phenylglucosides since glycoside analogues such as FPITC do not inhibit (Fig. 1*B*). At least for short times of expo-

sure, these inhibitors are fully reversible. However, in the case of the GPITC, longer exposure produces irreversible inhibition. Since isothiocyanates have been used to specifically label proteins at lysine residues (Weber & Semenza, 1983), we performed an experiment with brush border membrane vesicles to determine whether a lysine is present near the glucose binding site. The protection of the GPITC inhibition by D-glucose in the presence of Na^+ suggests that a lysine is present approximately 8 Å from the pyranose binding pocket and may be the residue which was previously identified as being in or near the glucose binding site (Peerce & Wright, 1984).

The interactions of phenylglucosides with SGLT1 have been confirmed using charge transfer measurements. Both transported phenylglucosides and inhibitors block SGLT1 charge transfer to levels consistent with their apparent $K_{0.5}$s and K_is (Fig. 6), as reported for glucose and phlorizin (Loo et al., 1993), while salicin did not affect charge transfer. This shows that the substrates and inhibitors interact in a similar way with SGLT1.

Molecular Modeling and Chemical Analysis

To understand the structural requirements for transporter/blocker action, we have used computational chemistry methods and compared the 3-D structures of the β phenylglucosides. We were able to make this comparison since the position of the phenyl ring relative to the pyranose ring was similar for all of the phenyl-β-D-glucosides. Therefore, the side chain groups in the same position will interact with the same or neighboring amino acid residues of the protein.

That phenylglucosides are transported by SGLT1 has direct bearing on the architecture of the sugar binding site and on the conformational changes of the protein that are responsible for sugar translocation across the plasma membrane. First, recall the severe restrictions on the structure of monosaccharides transported by SGLT1. Only hexoses in the pyranoside ring conformation with an equatorial –OH group on C-2 are transported efficiently and bulky residues, e.g., $-CH_3$, are only tolerated at C-1 (*see* Kimmich, 1981; Hopfer, 1987). This, together with the observation that neither phenylmannoside nor phenylfucoside derivatives interact with SGLT1, demonstrates that the monosaccharide moiety and not the aglucone is the determinant of phenylglucoside interaction with SGLT1. That the phenyl-β-D-glucosides arbutin and helicin are transported suggests that the binding site and the conformational changes responsible for substrate transport must be able to accommodate large molecules that can span at least one-third of the membrane (arbutin occupies a volume of ~10 × 5 × 5 Å). Comparably, mutants of *Lactose permease* have been shown to transport substrates spanning the entire thickness of the bilayer (Olsen, Green & Brookes, 1983). It is also clear that the structure of the aglucone determines whether or not a glucoside is a transported substrate, a blocker or a noninteracting sugar. A *para* –OH group on the phenyl ring increases the apparent affinity for transport, $-NO_2$ or –NCS group in the same position converts the phenyl glucoside to a blocker and an *ortho* $-CH_2OH$ eliminates interaction with the protein. Inspection of the 3-D structures of the phenyl-β-D-glucosides indicates that all have a very similar structures (Fig. 9). In contrast, the 3-D structures of glucosides which do not interact with SGLT1, e.g., lactose, trehalose and phenyl-α-D-glucosides, do not superimpose. There are substantial differences among the 3-D structures of the β and α phenylglucosides and disaccharides. Particularly, the phenyl ring of the α-phenylglucosides and the second pyranose ring of the disaccharides are perpendicular to the plane of the β-phenylglucoside rings (*not shown*). In contrast, *Lactose permease* transports α-nitrophenyl-galactosides even better than the β ones (Olsen & Brooker, 1989). This shows that the vestibule to the sugar binding site of SGLT1 imposes steric constraints to substrate access. In the case of PG, the phenyl ring probably interacts with the residues in the vestibule through both hydrophilic and/or π-electron hydrogen bonding. Addition of the *para* –OH group to the phenyl ring in arbutin increases the affinity for SGLT1 fivefold, probably through H-bonding with neighboring polar residues. One may be a lysine residue, since isothiocyanate analogues (GPITC) can irreversible inhibit SGLT1 (Fig. 7) and PITC is known to covalently react with lysine residues in proteins (Weber & Semenza, 1983). On the other hand, the potent reversible short-term inhibition observed with GPITC may be due to increased hydrophobic bonding (note that the octanol/water partition coefficient of PITC is greater than that for phenyl, Hansch & Leo, 1979).

In GSA, the phenyl ring is displaced one bond length more distant by the nitrogen bridge between glycosidic O and the phenyl ring, so that it does not superimpose with the phenyl ring of the other phenylglucosides (Fig. 9*C*). The potential for hydrogen bonding is high, but as the interaction of GSA with SGLT1 is very poor, stabilizing effects due to these interactions must be absent. It is possible that the lack of influence of the groups further out in the *para* position indicates that they are not closely associated with the protein, that is, they essentially remain in the aqueous medium. NPG and arbutin have similar structures, closely superimpose (Fig. 9*B*), and potentially have the ability of H-bonding; hence, we would expect NPG to be transported, nevertheless it behaves as a weak blocker (apparent K_i ~20 mM). Probably $-NO_2$ and –OH groups interact differently with the polar residues at close locations in the transporter as NPG can only accept H-bond whereas arbutin can both accept and donate. With the addition of the –CHO group to the

ortho position of the phenyl ring (Fig. 9*A*), apparent $K_{0.5}$ decreases to 14 mM (helicin). However, the $-CH_2OH$ group in the same position (salicin) impedes interaction of the phenylglucoside with the transporter. It is probable that this location in SGLT1 corresponds to a hydrophobic pocket where hydrogen bonding is limited. The difference in activity between salicin and helicin might then be explained if a hydrogen bond donor, but not an acceptor, is present at the active site. On the other hand, steric effects may play a role making this position an unfavorable location for interacting with SGLT1. As with helicin, phlorizin has a –CHO in the *ortho* position. Since helicin is a poor substrate, it is unlikely that –CHO at this location is important for the high affinity binding of phlorizin. Phlorizin is the classic high affinity inhibitor of SGLT1. It is subject to a keto-enol tautomerism, and examination of phlorizin using MM+ indicates that the lowest energy structure for the keto-phlorizin conformation places the second aromatic ring in a position such that it folds back over the first aromatic and pyranose rings (Fig. 9*D*), similar to a proposed structure for phloretin (Fuhrmann, Dernedde & Frenking, 1992). The results thus far suggest that the position of the second ring also accounts for the high affinity of keto-phlorizin for SGLT1, probably through a H-bond between the *para* –OH group and a polar residue in the transporter (Diedrich, 1990), whereas the enol-form is a much poorer inhibitor (B.A. Hirayama, *unpublished*). In folding back upon itself, phlorizin presents a much more bulky cross-section, and this may also account for its inability to be transported.

In rat intestine it has been reported that NPG is transported by SGLT1 (Mizuma et al., 1992) and salicin is an inhibitor of sugar "active" transport but is not transported (Alvarado & Crane, 1964). Preliminary experiments indicate that NPG is transported by rat SGLT1, and this demonstrates that small differences in amino acid sequence between rat and rabbit SGLT1 transporters produce differences in substrate specificity.

In conclusion, we have characterized a group of phenylglucosides as substrates, blockers and noninteracting sugars of the Na^+/glucose cotransporter. The differences in the phenylglucoside affinities for SGLT1 depending on the nature and position of the chemical groups in the phenyl ring, provide information about some structural requirements for binding to SGLT1, and establish a base for searching for other glucose-analogues with potential therapeutic effects that could use SGLT1 as an intestinal drug delivery system. Further studies of phenylglucoside interactions with SGLT1, using the approach outlined here, will provide novel information about the architecture of the vestibule to the sugar binding site and the conformational changes underlying the transport of the sugar across the membrane. Also, the use of these and other glucosides will permit us to investigate SGLT1 mutant selectivity and, hence, identify amino acid residues close to the glucose binding site.

We thank Dr. E. Turk for his helpful comments and review of the manuscript, Drs. K. Boorer and K. Hager for their technical assistance and our colleagues for their suggestions. M.P. Lostao was a recipient of a postdoctoral fellowship from the Health Department of Navarra Government, Spain. B.A. Hirayama was a recipient of a CURE pilot feasibility grant. This work was supported by National Institutes of Health grants NS 25554, DK 19567 and DK 44602.

References

Alvarado, F., Crane, R.K. 1964. Studies on the mechanism of intestinal absorption of sugars. VII. Phenylglycoside transport and its possible relationship to phlorizin inhibition of the active transport of sugars by the small intestine. *Biochim. Biophys. Acta* **93:**116–135

Birnir, B., Loo, D.D.F., Wright, E.M. 1991. Voltage-clamp studies of the Na^+/glucose cotransporter cloned from rabbit small intestine. *Pfluegers Arch.* **418:**79–85

Diedrich, D.F. 1990. Photoaffinity-labeling analogs of phlorizin and phloretin: synthesis and effect on cell membrane. *In:* Methods in Enzymology. Volume 191, pp. 755–780. Academic, New York

Fuhrmann, G.F., Dernedde S., Frenking, G. 1992. Phloretin keto-enol tautomerism and inhibition of glucose transport in human erythrocytes (including effects of phloretin on anion transport). *Biochim. Biophys. Acta* **1110:**105–111

Hansch, C., Leo, A. 1979. *In:* Substituent Constants for Correlation Analysis in Chemistry and Biology. Wiley-Interscience, New York

Hediger, M.A., Coady, M.J., Ikeda, T.S., Wright, E.M. 1987. Expression cloning and cDNA sequencing of the Na^+/glucose cotransporter. *Nature* **330:**379–381

Hopfer, U. 1987. Membrane transport mechanisms for hexoses and amino acids in the small intestine. *In:* Physiology of the Gastrointestinal Tract. Leonard R. Johnson, editor. pp. 1499–1526. Raven, New York

Ikeda, T.S., Hwang, E.-S., Coady, M.J., Hirayama, B.A., Hediger, M.A., Wright, E.M. 1989. Characterization of a Na^+/glucose cotransporter cloned from rabbit small intestine. *J. Membrane Biol.* **110:**87–95

Kimmich, G.A. 1981. Intestinal absorption of sugar. *In:* Physiology of the Gastrointestinal Tract. Leonard R. Johnson, editor. pp. 1035–1061. Raven, New York

La Course, W.R., Mead, D.A., Jr., Johnson, D.C. 1990. Anion-exchange separation of carbohydrates with pulsed amperometric detection using a pH-selective reference electrode. *Anal. Chem.* **62:**220–224

Landau, B.R., Bernstein, L., Wilson, T.H. 1962. Hexose transport by hamster intestine *in vitro*. *Am. J. Physiol.* **203:**237–240

Loo, D.D.F., Hazama, A., Supplisson, S., Turk, E., Wright, E.M. 1993. Relaxation kinetics of the Na^+/glucose cotransporter. *Proc. Natl. Acad. Sci. USA* **90:**5767–5771

Mizuma, T., Ohta, K., Hayashi, M., Awazu, S. 1992. Intestinal active absorption of sugar-conjugate compounds by glucose transport system: implication of improvement of poorly absorbable drugs. *Biochem. Pharmacol.* **43:**2037–2039

Mopper, K., Schultz, C.A., Chevolot, L., Germain, C., Revuelta, R., Dawnson, R. 1992. Determination of sugars in concentrated seawater and other natural waters by liquid chromatography and pulsed amperometric detection. *Environ. Sci. Technol.* **26:**133–138

Olsen, S.G., Brooker, R.J. 1989. Analysis of the structural specificity of the Lactose Permease toward sugars. *J. Biol. Chem.* **264:**15982–15987

Olsen, S.G., Greene, K.M., Brooker, R.J. 1993. Lactose Permease mutants which transport (malto-)oligosaccharides. *J. Bacteriol.* **175:**6269–6275

Parent, L., Supplisson, S., Loo, D.D.F., Wright, E.M. 1992*a*. Electrogenic properties of the cloned Na^+/glucose cotransporter: I. Voltage-clamp studies. *J. Membrane Biol.* **125:**49–62

Parent, L., Supplisson, S., Loo, D.D.F., Wright, E.M. 1992*b*. Electrogenic properties of the cloned Na^+/glucose cotransporter: II. A transport model under nonrapid equilibrium conditions. *J. Membrane Biol.* **125:**63–79

Peerce, B.E., Wright, E.M. 1984. Conformational changes in the intestinal brush border sodium-glucose cotransporter labeled with fluorescein isothiocyanate. *Proc. Natl. Acad. Sci. USA* **81:**2223–2226

Stevens, B.R., Ross, H.J., Wright, E.M. 1982. Multiple transport pathways for neutral amino acids in rabbit jejunal brush border vesicles. *J. Membrane Biol.* **66:**213–225

Umbach, J.A., Coady, M.J., Wright, E.M. 1990. Intestinal Na^+/glucose cotransporter expressed in *Xenopus* oocytes is electrogenic. *Biophys. J.* **57:**1217–1224

Weber, J., Semenza, G. 1983. Chemical modification of the small intestinal Na^+/glucose cotransporter by amino group reagents. Evidence for a role of amino group(s) in the binding of the sugar. *Biochem. Biophys. Acta.* **731:**437–447

Zampighi, G.A., Boorer, J.K., Kreman, M., Loo, D.D.F., Wright, E.M. 1994. Freeze-fracture of the Na/glucose cotransporter (SGLT1) expressed in *Xenopus* oocytes. *FASEB J.* **8:**342 (*Abstr.*)